Inorg. Chem. **2005**, *44*, 9506–9517

Coupling of an Aldehyde or Ketone to Pyridine Mediated by a Tungsten Imido Complex

Trevor W. Hayton,[†] James M. Boncella,*[,†] Brian L. Scott,[†] Khalil A. Abboud,[‡] and Ryan C. Mills[‡]

Chemistry Division, Los Alamos National Laboratory, P.O. Box 1663, MS J582, Los Alamos, New Mexico 87545, and Department of Chemistry and Center for Catalysis, University of Florida, Gainesville, Florida 32611-7200

Received July 8, 2005

The reactivity of W(NPh)(*o*-$(Me_3SiN)_2C_6H_4$)$(py)_2$ and W(NPh)(*o*-$(Me_3SiN)_2C_6H_4$)$(pic)_2$ (py = pyridine; pic = 4-picoline) with unsaturated substrates has been investigated. Treatment of W(NPh)(*o*-$(Me_3SiN)_2C_6H_4$)$(py)_2$ with diphenylacetylene or 2,3-dimethyl-1,3-butadiene generates W(NPh)(*o*-$(Me_3SiN)_2C_6H_4$)(η^2-PhC≡CPh) (**1**) and W(NPh)(*o*-$(Me_3SiN)_2C_6H_4$)-(η^4-CH_2═C(Me)C(Me)═CH_2) (**3**), respectively, while the addition of ethylene to W(NPh)(*o*-$(Me_3SiN)_2C_6H_4$)$(py)_2$ generates the known metallacycle W(NPh)(*o*-$(Me_3SiN)_2C_6H_4$)($CH_2CH_2CH_2CH_2$). The addition of 2 equiv of acetone to W(NPh)(*o*-$(Me_3SiN)_2C_6H_4$)$(pic)_2$ provides the azaoxymetallacycle W(NPh)(*o*-$(Me_3SiN)_2C_6H_4$)$(OCH(Me)_2)$($OC(Me)_2$-*o*-C_5H_3N-*p*-Me) (**4**), the result of acetone insertion into the ortho C–H bond of picoline. Similarily, the addition of 2 equiv of RC(O)H [R = Ph, ^{t}Bu] to W(NPh)(*o*-$(Me_3SiN)_2C_6H_4$)$(py)_2$ generates W(NPh)(*o*-$(Me_3SiN)_2C_6H_4$)(OCH_2R)-($OCH(R)$-*o*-C_5H_4N) [R = Ph, **5**; ^{t}Bu, **6**]. In contrast, reaction between W(NPh)(*o*-$(Me_3SiN)_2C_6H_4$)$(py)_2$ and 2-pyridine carboxaldehyde yields the diolate W(NPh)(*o*-$(Me_3SiN)_2C_6H_4$)($OCH(C_5H_4N)CH(C_5H_4N)O$) (**7**). The synthesis of W(NPh)-(*o*-$(Me_3SiN)_2C_6H_4$)$(PMe_3)(py)$(η^2-OC(H)C_6H_4-*p*-Me) (**9**), formed by the addition of *p*-tolualdehyde to a mixture of W(NPh)(*o*-$(Me_3SiN)_2C_6H_4$)$(py)_2$ and PMe_3, suggests that an η^2-aldehyde intermediate is involved in the formation of the azaoxymetallacycle, while the isolation of W(NPh)(*o*-$(Me_3SiN)_2C_6H_4$)(Cl)($OC(Me)(CMe_3)$-*o*-C_5H_4N) (**10**), formed by the reaction of pinacolone with W(NPh)(*o*-$(Me_3SiN)_2C_6H_4$)$(py)_2$, in the presence of adventitious CH_2Cl_2, suggests that the reaction proceeds via the hydride W(NPh)(*o*-$(Me_3SiN)_2C_6H_4$)(H)($OC(Me)(CMe_3)$-*o*-C_5H_4N).

Introduction

Electrophilic aromatic substitution is generally a very effective way of functionalizing an aromatic ring.[1] However, with heterocycles such as pyridine, the electron-poor nature of the ring makes electrophilic aromatic substitution nonviable, and other synthetic strategies must be employed. In this regard, metal-mediated transformations are particularly attractive, and a number of metal-based routes for functionalizing heterocyclic ring systems are known. For instance, the silaacyl carbon of Cp*$TaCl_3$(η^2-CO$(SiMe_3)(PR_3)$) inserts into the C−H bond of pyridine to form Cp*$TaCl_3$($OCH(SiMe_3)$-*o*-C_5H_4N).[2,3] Similarly, Cp*Lu(bipy)$(CH_2SiMe_3)_2$ reacts with CO to give an azaoxymetallacycle through cleavage of the ortho C−H bond of the bipy ligand.[4] Rothwell and co-workers have also documented the ortho C−H activation of a coordinated pyridine.[5,6] The zirconocene complexes studied by Jordan and co-workers have also yielded interesting results.[7,8] For instance, the addition of alkenes to $Cp_2Zr(\eta^2$-pyridyl$)(THF)^+$ generates five-membered azazirconcycles such as $Cp_2Zr\{(\eta^2$-*C*,*N*-$CH_2CH(Me)$-(2-Me-6-pyridyl)$\}^+$.[9,10] In the presence of H_2, this complex catalyzes the insertion of propene into the ortho C−H bond

* To whom correspondence should be addressed. E-mail: boncella@lanl.gov.
[†] Los Alamos National Laboratory.
[‡] University of Florida.

(1) March, J. *Advance Organic Chemistry*, 4th ed.; John Wiley & Sons: New York, 1992; pp 501−568.
(2) Arnold, J.; Tilley, T. D.; Rheingold, A. L.; Geib, S. J.; Arif, A. M. *J. Am. Chem. Soc.* **1989**, *111*, 149−164.
(3) Arnold, J.; Woo, H.-G.; Tilley, T. D.; Rheingold, A. L.; Geib, S. J. *Organometallics* **1988**, *7*, 2045−2049.
(4) Cameron, T. M.; Gordon, J. C.; Scott, B. L.; Tumas, W. *J. Chem. Soc., Chem. Commun.* **2004**, 1398−1399.
(5) Zambrano, C. H.; McMullen, A. K.; Kobriger, L. M.; Fanwick, P. E.; Rothwell, I. P. *J. Am. Chem. Soc.* **1990**, *112*, 6565−6570.
(6) Fanwick, P. E.; Kobriger, L. M.; McMullen, A. K.; Rothwell, I. P. *J. Am. Chem. Soc.* **1986**, *108*, 8095−8097.
(7) Guram, A. S.; Jordan, R. F. *Organometallics* **1991**, *10*, 3470−3479.
(8) Rodewald, S.; Jordan, R. F. *J. Am. Chem. Soc.* **1994**, *116*, 4491−4492.
(9) Bi, S.; Lin, Z.; Jordan, R. F. *Organometallics* **2004**, *23*, 4882−4890.
(10) Jordan, R. F.; Taylor, D. F. *J. Am. Chem. Soc.* **1989**, *111*, 778−779.

10.1021/ic0511367 CCC: $30.25
Published on Web 11/15/2005

of 2-picoline to generate 2-methyl-6-isopropylpyridine, a transformation that mirrors Friedel−Crafts chemistry.

Recent work in our laboratories has focused on the chemistry of W(NPh)(*o*-$(Me_3SiN)_2C_6H_4$)$(py)_2$ and W(NPh)(*o*-$(Me_3SiN)_2C_6H_4$)$(pic)_2$ (py = pyridine; pic = 4-picoline). These unique, square-pyramidal imido complexes exhibit hindered rotation about their W−N(pyridine) bonds. They also readily react with Lewis bases to generate six-coordinate compounds. For instance, W(NPh)(*o*-$(Me_3SiN)_2C_6H_4$)$(py)_2$ forms the carbonyl complex W(NPh)(*o*-$(Me_3SiN)_2C_6H_4$)$(py)_2$(CO) when exposed to carbon monoxide and forms W(NPh)(*o*-$(Me_3SiN)_2C_6H_4$)(py)$(PMe_3)_2$ when treated with trimethylphosphine.[11] Furthermore, W(NPh)(*o*-$(Me_3SiN)_2C_6H_4$)$(py)_2$ inserts into the C−S bond of thiophene upon thermolysis to produce the six-membered metalathiocycle W(NPh)(*o*-$(Me_3SiN)_2C_6H_4$)(SC_4H_4).[12] Given these interesting results, the reactivity of W(NPh)(*o*-$(Me_3SiN)_2C_6H_4$)$(py)_2$ and W(NPh)(*o*-$(Me_3SiN)_2C_6H_4$)$(pic)_2$ with other potential ligands and substrates was studied.

In this contribution, we describe the reactivity of W(NPh)(*o*-$(Me_3SiN)_2C_6H_4$)$(py)_2$ and W(NPh)(*o*-$(Me_3SiN)_2C_6H_4$)$(pic)_2$ with alkenes, diphenylacetylene, acetone, and aldehydes. With alkenes and diphenylacetylene, substitution of the two heterocyclic ligands occurs to give the corresponding π-bound olefin or acetylene adducts. With acetone or aldehydes, however, insertion of the carbonyl group of these substrates into the ortho C−H bond of pyridine (or picoline) is observed.

Results

Synthesis and Characterization of W(NPh)(*o*-$(Me_3SiN)_2C_6H_4$)(η^2-PhC≡CPh). Heating a solution containing equimolar amounts of W(NPh)(*o*-$(Me_3SiN)_2C_6H_4$)$(py)_2$ and diphenylacetylene to 55 °C for 4 h generates a brown-yellow solution. From this solution, W(NPh)(*o*-$(Me_3SiN)_2C_6H_4$)(η^2-PhC≡CPh) (**1**) can be isolated in 68% yield as an air- and moisture-sensitive brown powder (eq 1). The ^{1}H NMR spectrum of **1** is consistent with the presence of a diphenylacetylene moiety and contains no signals attributable to a coordinated pyridine, while the $^{13}C\{^1H\}$ NMR spectrum exhibits a singlet at 198.5 ppm, which is assigned to the alkyne carbons of the diphenylacetylene ligand.

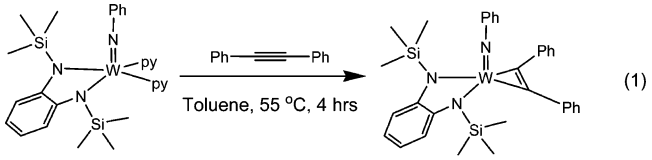

(1)

1

Single crystals of **1** were grown from an Et_2O solution stored at −40 °C for several weeks and were analyzed by X-ray crystallography. The solid-state molecular structure of **1** is shown in Figure 1. Compound **1** adopts a distorted square-pyramidal geometry with the imido ligand in the apical position. Both the W−N1(imido) distance [1.756(2) Å] and W−N1(imido)−C1 angle [161.8(2)°] are similar to those seen in other members of this class of compounds.[11] As well, the phenylenediamide ligand exhibits metrical parameters characteristic of that ligand. In particular, the fold angle (the angle between the phenylenediamide aryl ring and the N2−W−N3 plane) is 135°, which is similar to the angle found in the related molybdenum alkyne complex Mo(NPh)(*o*-$(Me_3SiN)_2C_6H_4$)(η^2-$(Me_3Si)C{\equiv}C(SiMe_3)$).[13] The W−C19 and W−C20 bond lengths [both 2.054(3) Å] are in the range of W−C single bonds, while the C19−C20 distance [1.332(4) Å] is in the range of a C=C bond. This evidence suggests that a metallacyclopropene structure best describes the bonding of the acetylene ligand in **1**.

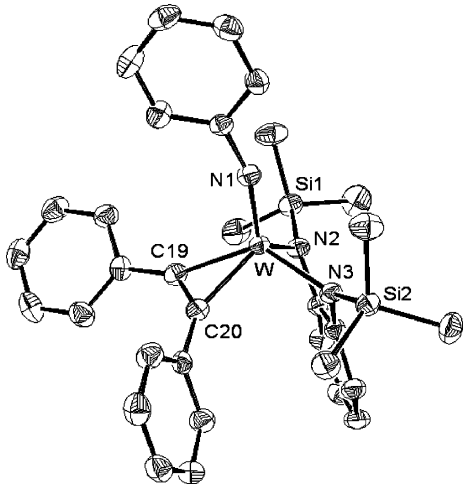

Figure 1. ORTEP diagram of W(NPh)(*o*-$(Me_3SiN)_2C_6H_4$)(η^2-PhC≡CPh) (**1**) with 50% probability ellipsoids being shown. Selected bond lengths (Å) and angles (deg): W−N1 = 1.756(2), W−N2 = 1.984(2), W−N3 = 2.017(2), W−C19 = 2.054(3), W−C20 = 2.054(3), C19−C20 = 1.332(4), C1−N1−W = 161.8(2).

Reactions of W(NPh)(*o*-$(Me_3SiN)_2C_6H_4$)$(py)_2$ with Olefins. Toluene solutions of W(NPh)(*o*-$(Me_3SiN)_2C_6H_4$)$(py)_2$ react with ethylene (20 psi) over 30 min, giving yellow-brown solutions containing the previously known compound W(NPh)(*o*-$(Me_3SiN)_2C_6H_4$)($CH_2CH_2CH_2CH_2$) (**2**) (Scheme 1).[14] Complex **2** can be isolated in 66% yield with this procedure. The previous synthetic method involved the reaction of W(NPh)(*o*-$(Me_3SiN)_2C_6H_4$)Cl_2 with $BrMg(CH_2)_4MgBr$ in Et_2O.[14] Similarly, toluene solutions of W(NPh)(*o*-$(Me_3SiN)_2C_6H_4$)$(py)_2$ also react with 1 equiv of 2,3-dimethyl-1,3-butadiene when heated to 60 °C for 20 h to give red-brown solutions containing W(NPh)(*o*-$(Me_3SiN)_2C_6H_4$)(η^4-$CH_2{=}C(Me)C(Me){=}CH_2$) (**3**) (Scheme 1).

Complex **3** can be isolated as a dark brown solid in 73% yield. This compound exhibits two doublets at 1.31 and 2.17 ppm in its ^{1}H NMR spectrum, which can be assigned to the two diastereotopic protons attached to the α carbons of the coordinated butadiene ligand. The resonances of these carbons are observed at 50.5 ppm in the ^{13}C NMR spectrum

(11) Mills, R. C.; Wang, S. Y. S.; Abboud, K. A.; Boncella, J. M. *Inorg. Chem.* **2001**, *40*, 5077−5082.
(12) Mills, R. C.; Abboud, K. A.; Boncella, J. M. *J. Chem. Soc., Chem. Commun.* **2001**, 1506−1507.
(13) Ison, E. A.; Cameron, T. M.; Abboud, K. A.; Boncella, J. M. *Organometallics* **2004**, *23*, 4070−4076.
(14) Wang, S.-Y. S.; VanderLende, D. D.; Abboud, K. A.; Boncella, J. M. *Organometallics* **1998**, *17*, 2628−2635.

Scheme 1

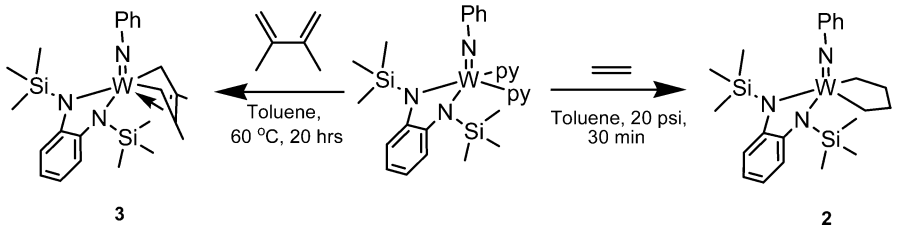

and exhibit a one-bond $^{13}C-^{1}H$ coupling constant of 143 Hz. The NMR data suggest that the α carbons of the butadiene ligand have considerable sp^3 character, and consequently, the $\sigma_2\pi$ resonance form predominates.[15] To confirm this feature, an X-ray crystallographic study of complex **3** was undertaken.

Single crystals of **3** suitable for X-ray diffraction analysis were grown from a pentane solution stored at −40 °C. Complex **3** crystallizes in the triclinic space group $P\bar{1}$ with two independent molecules in the asymmetric unit. The solid-state molecular structure of one of these is shown in Figure 2. Complex **3** adopts a distorted square-pyramidal geometry about W with the imido group occupying the apical position. The metrical parameters of the imido ligand [W−N1 = 1.755(3) Å, W−N1−C1 = 169.3(3)°] are similar to those observed in **1**. The di(amido) chelate, however, exhibits slightly longer W−N bond lengths [W−N2 = 2.040 (3) Å, W−N3 = 2.045(3) Å] and a more planar phenylenediamide ligand (fold angle 149°). The bond distances associated with the butadiene fragment are consistent with the NMR data and support the $\sigma_2\pi$ bonding model. For instance, the $C_\alpha-C_\beta$ bond lengths are 1.475(7) and 1.472(7) Å, while the $C_\beta-C_\beta$ bond length is 1.375(7) Å. Furthermore, the $W-C_\alpha$ bond lengths[W−C19 = 2.183(5) Å, W−C22 = 2.178(5) Å] are shorter than the $W-C_\beta$ bond lengths [W−C20 = 2.460(4) Å, W−C21 = 2.459(5) Å]. These parameters are similar to those found in Cp_2Zr(2,3-dimethylbutadiene), which is often considered the quintessential example of a $\sigma_2\pi$-bound butadiene complex.[16]

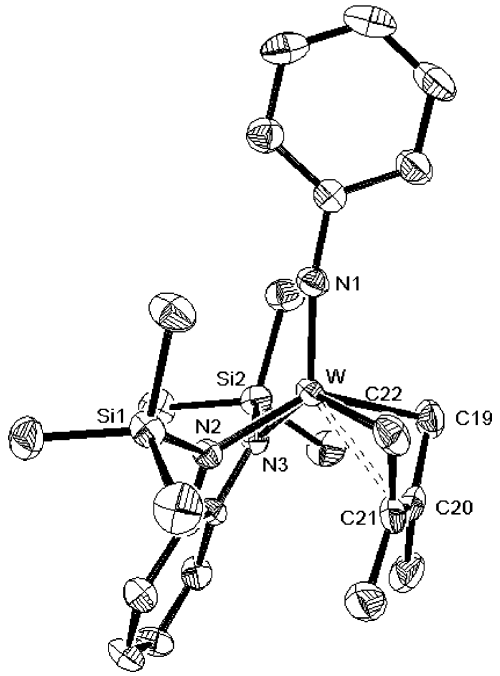

Figure 2. ORTEP diagram of W(NPh)(*o*-$(Me_3SiN)_2C_6H_4$)(η^4-CH_2═C(Me)C(Me)═CH_2) (**3**) with 50% probability ellipsoids being shown. Selected bond lengths (Å) and angles (deg): W−N1 = 1.755(3), W−N2 = 2.040(3), W−N3 = 2.045(3), W−C22 = 2.178(5), W−C19 = 2.183(5), W−C21 = 2.459(5), W−C20 = 2.460(4), C19−C20 = 1.475(7), C20−C21 = 1.375(7), C21−C22 = 1.472(7), W−N1−C1 = 169.3(3).

Synthesis and Characterization of W(NPh)(*o*-$(Me_3SiN)_2C_6H_4$)(OCH(Me)$_2$) (*O*C(Me)$_2$-*o*-C_5H_3N-*p*-Me). We attempted to extend the substitution chemistry of W(NPh)(*o*-$(Me_3SiN)_2C_6H_4$)$(py)_2$ and W(NPh)(*o*-$(Me_3SiN)_2C_6H_4$)$(pic)_2$ to other unsaturated organic molecules. Thus, W(NPh)(*o*-$(Me_3SiN)_2C_6H_4$)$(pic)_2$ rapidly reacts with acetone to form deep-green solutions, which turn orange-brown upon standing. Crystallization of the reaction residue from pentane provides orange crystals of W(NPh)(*o*-$(Me_3SiN)_2C_6H_4$)-(OCH(Me)$_2$)(*O*C(Me)$_2$-*o*-C_5H_3N-*p*-Me) (**4**) in 18% yield (eq 2). The ^{1}H NMR spectrum of **4** is consistent with the proposed formulation. For instance, a septet at 4.93 ppm (1H, J_{HH} = 6 Hz) and a doublet at 1.11 ppm (6H, J_{HH} = 6 Hz) indicates the presence of an isopropoxide ligand, while a prominent doublet at 8.18 ppm (assignable to the picoline ring ortho proton) demonstrates that picoline is incorporated into the final product.

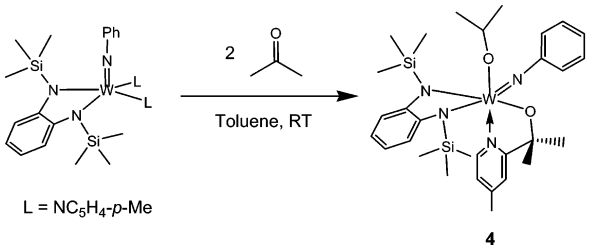

(2)

Single crystals of **4** were grown from a concentrated pentane solution. The solid-state molecular structure of **4** is shown in Figure 3. Complex **4** adopts an octahedral geometry about tungsten. Interestingly, one arm of the phenylenediamide ligand is trans to the imido ligand, a rare structural feature in this class of compounds.[17] The imido ligand [W−N1 = 1.763(7) Å, W−N1−C1 = 169.4(6)°] exhibits parameters similar to those seen in **1** and **3**. The two amido

(15) Yasuda, H.; Tatsumi, K.; Okamoto, T.; Mashima, K.; Lee, K.; Nakamura, A.; Kai, Y.; Kanehisa, N.; Kasai, N. *J. Am. Chem. Soc.* **1985**, *107*, 2410−2422.
(16) Yasuda, H.; Tatsumi, K.; Nakamura, A. *Acc. Chem. Res.* **1985**, *18*, 120−126.
(17) Boncella, J. M.; Wang, S. Y. S.; VanderLende, D. D.; Huff, R. L.; Abboud, K. A.; Vaughn, W. M. *J. Organomet. Chem.* **1997**, *530*, 59−70.

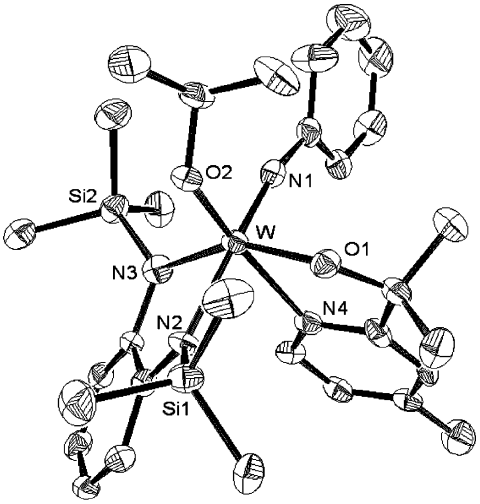

Figure 3. ORTEP diagram of W(NPh)(*o*-$(Me_3SiN)_2C_6H_4$)($OCMe_2$)-(*O*$C(Me)_2$-*o*-C_5H_3N-*p*-Me) (**4**) with 50% probability ellipsoids being shown. Selected bond lengths (Å) and angles (deg): W−N1 = 1.763(7), W−O2 = 1.874(6), W−O1 = 1.929(5), W−N3 = 2.005(7), W−N2 = 2.152(6), W−N4 = 2.293(7), W−N1−C1 = 169.4(6).

groups of the phenylenediamide ligand exhibit different W−N distances [W−N3 = 2.005(7) Å, W−N2 = 2.152(6) Å], a manifestation of the trans influence as the amide nitrogen with the longer W−N bond (N2) is trans to the imido ligand.[18] The W−O(isopropoxide) distance [W−O2 = 1.874(6) Å] is similar to those found in related complexes.[19]

The most interesting structural feature in **3** is the five-membered azaoxymetallacycle, formed by the coupling of picoline with acetone. The W−N(picoline) bond length is 2.293(7) Å, much longer than that seen in the parent compound W(NPh)(*o*-$(Me_3SiN)_2C_6H_4$)$(pic)_2$ [W−N(picoline) = 2.083(3) Å and 2.109(3) Å] but consistent with other W−N(py) bond lengths,[20,21] while the W−O1 bond length of 1.929(5) Å is comparable to those seen in similar compounds.[22]

Synthesis and Characterization of W(NPh)(*o*-$(Me_3SiN)_2C_6H_4$)(OCH_2R)(*O*CH(R)-*o*-C_5H_4N) [R = Ph, ^{t}Bu]. The tungsten(IV) pyridine complex was also found to react with aldehydes. the addition of 2 equiv of benzaldehyde or trimethylacetaldehyde to W(NPh)(*o*-$(Me_3SiN)_2C_6H_4$)$(py)_2$ at room temperature generates solutions containing W(NPh)-(*o*-$(Me_3SiN)_2C_6H_4$)(OCH_2R)(*O*CH(R)-*o*-C_5H_4N) [R = Ph, **5**; ^{t}Bu, **6**] (eq 3). Crystallization from pentane provides **5** and **6** as red crystalline materials in 36% and 21% yields, respectively.

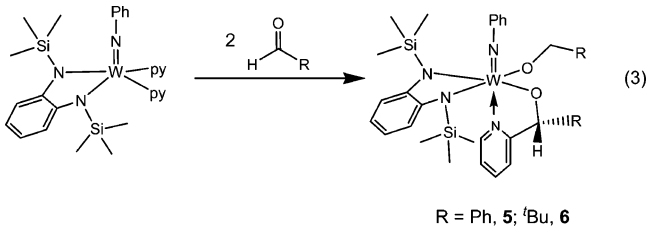

(3)

R = Ph, **5**; ^{t}Bu, **6**

Both **5** and **6** display several characteristic signals in their respective ^{1}H NMR spectra that support the proposed formulation. For instance, the diastereotopic protons of the benzyl alkoxide ligand in **5** appear as two doublets at 5.65 and 5.89 ppm ($^2J_{HH}$ = 14 Hz), while the lone proton attached to the carbonyl carbon of the metallacycle appears as a singlet at 6.46 ppm. In **6**, the signals for the diastereotopic protons of the neopentoxide ligand are found at 4.19 and 4.34 ppm ($^2J_{HH}$ = 11 Hz), and the proton attached to the carbonyl carbon of the metallacycle appears at 5.20 ppm. As with the ^{1}H NMR spectrum of **4**, a prominent multiplet corresponding to the ortho proton of the pyridine ring is found at a significantly downfield chemical shift: 8.41 ppm for **5** and 8.32 ppm for **6**. Interestingly, the ^{1}H NMR spectra of **5** and **6** are consistent with the presence of only one diastereomer.

Single crystals of **6** suitable for X-ray diffraction analysis were grown from a saturated pentane solution stored at −30 °C. The solid-state molecular structure of **6** is shown in Figure 4. Complex **6** crystallizes in the triclinic space group $P\bar{1}$ as the pentane solvate **6**·$^1/_2C_5H_{12}$. The complex adopts an octahedral geometry around W, with the imido ligand trans to the functionalized pyridine. The imido ligand [W1−N4 = 1.751(2) Å, W1−N4−C1 = 172.4(2)°] exhibits the expected metrical parameters, while the phenylenediamide W−N distances [W1−N2 = 2.031(2) Å, W1−N1 = 2.082-(2) Å] are similar to those observed for **1** and **3**. The two W−O distances are similar [W1−O1 = 1.931(2) Å, W1−O2 = 1.950(2) Å] and compare favorably to other W−O(alkoxide) distances.[19] The W−N(pyridine) distance [W1−N3 = 2.313(2) Å] is similar to that observed in **4**, while the *tert*-butyl group of the metallacycle is syn to the alkoxide ligand.

Isolation of W(NPh)(*o*-$(Me_3SiN)_2C_6H_4$)(*O*$CH(C_5H_4N)$-$CH(C_5H_4N)O$). During an attempt to extend the scope of this reaction to other aldehydes, a few red crystals were isolated from the reaction between W(NPh)(*o*-$(Me_3SiN)_2C_6H_4$)-$(py)_2$ and 2-pyridine carboxaldehyde. Crystals suitable for X-ray diffraction were grown from Et_2O, and X-ray crystallography revealed these crystals to be W(NPh)(*o*-$(Me_3SiN)_2C_6H_4$)(*O*$CH(C_5H_4N)CH(C_5H_4N)O$) (**7**). The solid-state molecular structure of **7** is shown in Figure 5. Complex **7** evidently results from the displacement of both pyridine ligands and the subsequent coupling of two aldehyde fragments to generate the W(VI) diolate complex, **7** (eq 4).

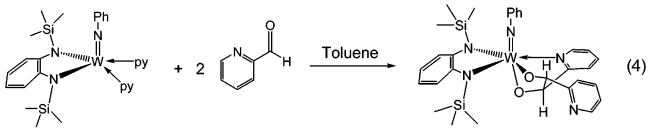

(4)

7

In addition, one of the 2-pyridine substituents is coordinated to the tungsten to form a unique O_2N tridentate ligand. The W1−N1−C1 angle of the imido ligand is 155.1(4)°,

(18) Coe, B. J.; Glenwright, S. J. *Coord. Chem. Rev.* **2000**, *203*, 5−80.
(19) Schrock, R. R.; DePue, R. T.; Feldman, J.; Schaverien, C. J.; Dewan, J. C.; Liu, A. H. *J. Am. Chem. Soc.* **1988**, *110*, 1423−1435.
(20) Kriley, C. E.; Fanwick, P. E.; Rothwell, I. P. *J. Am. Chem. Soc.* **1994**, *116*, 5225−5232.
(21) Wesemann, L.; Waldmann, L.; Ruschewitz, U.; Ganter, B.; Wagner, T. *J. Chem. Soc., Dalton Trans.* **1997**, 1063−1068.
(22) van der Schaaf, P. A.; Abbenhuis, R. A. T. M.; Grove, D. M.; Smeets, W. J. J.; Spek, A. L.; van Koten, G. *J. Chem. Soc., Chem. Commun.* **1993**, 504−506.

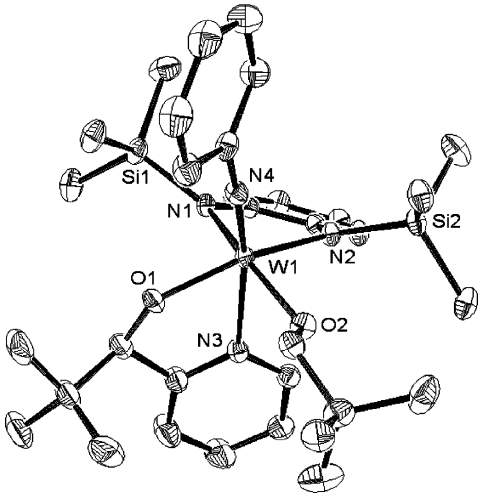

Figure 4. ORTEP diagram of W(NPh)(*o*-$(Me_3SiN)_2C_6H_4$)(OCH_2CMe_3)(*O*CH(CMe_3)-*o*-C_5H_4N) (**6**) with 50% probability ellipsoids being shown. Selected bond lengths (Å) and angles (deg): W1−N4 = 1.751(2), W1−O1 = 1.931(2), W1−O2 = 1.950(2), W1−N2 = 2.031(2), W1−N1 = 2.082(2), W1−N3 = 2.313(2), W1−N4−C1 = 172.4(2).

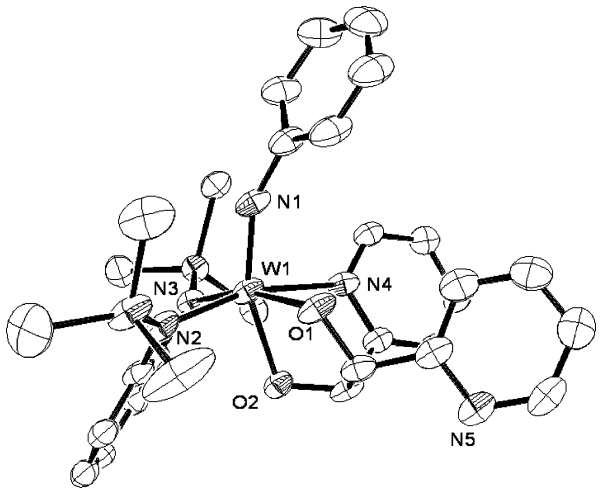

Figure 5. ORTEP diagram of W(NPh)(*o*-$(Me_3SiN)_2C_6H_4$)(*O*CH(C_5H_4N)-CH(C_5H_4N)*O*) (**7**) with 50% probability ellipsoids being shown. Selected bond lengths (Å) and angles (deg): W1−N1 = 1.775(5), W1−N2 = 2.007-(5), W1−O1 = 2.012(4), W1−O2 = 2.020(4), W1−N3 = 2.026(5), W1−N4 = 2.262(5), W1−N1−C1 = 155.1(4).

much smaller than that observed in similar imido complexes, while the fold angle of the phenylenediamide ligand (139.5°) is comparable to related compounds. The two W−O bond lengths [W1−O1 = 2.012(4) Å, W1−O2 = 2.020(4) Å] are identical but are slightly longer than the tungsten−alkoxide bond lengths observed in **4** and **6**. The W−N(pyridine) bond length is 2.262(5) Å and is close to that observed for **4**. Interestingly, the product is the *syn*-diol coupling product. Previously, coupling of benzaldehyde at Ti has yielded the *anti*-diolate product,[23] or mixtures of both anti and syn,[24] while the coupling of benzaldehyde with SmI_2/tetraglyme gives primarily the syn (or meso) diol.[25]

The ^{1}H NMR spectrum of compound **7** at room temperature consists of several broad singlets. However, its ^{1}H NMR spectrum at −30 °C in toluene-d_8 reveals the presence of two inequivalent trimethylsilyl groups, while two doublets at 8.40 and 8.51 ppm are assigned to the ortho protons of the pyridine substituents. There is no indication of the presence of the *anti*-diol diastereomer in the ^{1}H NMR spectrum. Warming a toluene-d_8 solution of **7** to 30 °C results in the coalescence of the inequivalent Me_3Si groups. The fluxionality can be explained by invoking pyridine dissociation from the metal to give a five-coordinate transition state. Coordination of the other pyridyl moiety regenerates the octahedral species (Scheme 2). Using the two-site exchange approximation, the activation barrier ($\Delta G_C^{\ddagger}$) was calculated to be 15.0 kcal mol^{-1} for this process.[26]

Labeling Studies. To understand how **4**, **5**, and **6** are formed, we undertook a number of deuterium labeling studies. Thus, the reaction of W(NPh)(*o*-$(Me_3SiN)_2C_6H_4$)(py-d_5)$_2$ with 2 equiv of benzaldehyde generates red solutions containing W(NPh)(*o*-$(Me_3SiN)_2C_6H_4$)(OCHDPh)(*O*CH(Ph)-*o*-C_5D_4N) (**5**-d_5). A ^{1}H NMR spectrum of **5**-d_5 displays two singlets at 5.63 and 5.89 ppm, in an 8:1 ratio, and not the doublet of doublets as was seen with **5**. Furthermore, the prominent multiplet observed at 8.41 ppm in the ^{1}H NMR spectrum of **5** is not observed in the ^{1}H NMR spectrum of **5**-d_5. The ^{2}H NMR spectrum of **5**-d_5 in C_6H_6 exhibits a broad singlet at 5.86 ppm and another broad singlet at 8.41 ppm.

This experiment demonstrates that one hydrogen on the alkoxide ligand originates from the pyridine ortho position (eq 5). It also reveals that the addition of the hydrogen to the aldehyde to form the alkoxide occurs in a diastereoselective fashion, as only one of the two hydrogen positions α to the oxygen becomes deuterated to any extent.

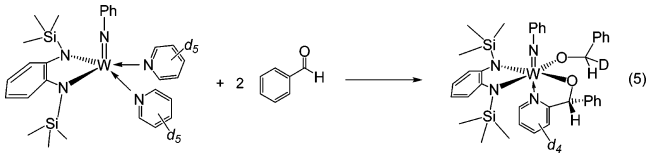

Similarly, the reaction of W(NPh)(*o*-$(Me_3SiN)_2C_6H_4$)(py-d_5)$_2$ with 2 equiv of trimethylacetaldehyde generates W(NPh)(*o*-$(Me_3SiN)_2C_6H_4$)(OCHDCMe_3)(*O*CH(CMe_3)-*o*-C_5D_4N) (**6**-d_5). As with the ^{1}H NMR spectrum of **5**-d_5, the ^{1}H NMR spectrum of **6**-d_5 exhibits two singlets at 4.15 and 4.32 ppm, in a ratio of 9:5, respectively, as opposed to the doublet of doublets seen in the protio analogue. This experiment is completely consistent with the benzaldehyde result; however, the reaction proceeds with significantly lower diastereoselectivity.

Finally, to determine if a kinetic isotope effect is involved in azaoxymetallacycle formation, W(NPh)(*o*-$(Me_3SiN)_2C_6H_4$)(py-2-d_1)$_2$ was synthesized from W(NPh)(*o*-$(Me_3SiN)_2C_6H_4$)Cl_2 and py-2-d_1. The reaction of W(NPh)(*o*-$(Me_3SiN)_2C_6H_4$)(py-2-d_1)$_2$ with 2 equiv of benzaldehyde or trimethylacetaldehyde generates W(NPh)(*o*-$(Me_3SiN)_2C_6H_4$)(OCH(H/D)R)-

(23) Steinhuebel, D. P.; Lippard, S. J. *J. Am. Chem. Soc.* **1999**, *121*, 11762−11772.
(24) Du, G.; Mirafzal, G. A.; Woo, L. K. *Organometallics* **2004**, *23*, 4230−4235.
(25) Aspinall, H. C.; Greeves, N.; Valla, C. *Org. Lett.* **2005**, *7*, 1919−1922.
(26) Friebolin, H. *Basic One- and Two-Dimensional NMR Spectroscopy*; VCH Publishers: New York, 1993; p 295.

Scheme 2

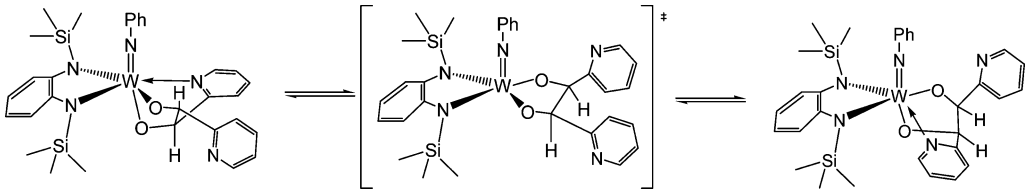

(*O*CH(R)-*o*-C_5H_3(H/D)*N*) (R = Ph, **5**-d_1; R = ^{t}Bu, **6**-d_1) (eq 6). In both products, the deuterium label was distributed equally between the ortho pyridine position and the methylene group of the alkoxide ligand. This result is consistent with a rate-determining step *that does not involve* pyridine C−H(D) bond cleavage.

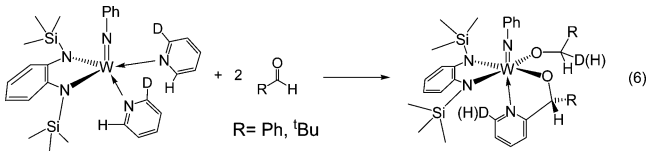

Synthesis of W(NPh)(*o*-(Me_3SiN)$_2C_6H_4$)(py)(PMe_3)(η^2-OC(H)R) [R = Ph, *p*-tol]. The reaction of W(NPh)(*o*-(Me_3SiN)$_2C_6H_4$)(py)$_2$ with benzaldehyde or *p*-tolualdehyde in the presence of trimethylphosphine does not yield an azaoxametallacycle-containing complex. Instead, W(NPh)(*o*-(Me_3SiN)$_2C_6H_4$)(py)(PMe_3)(η^2-OC(H)R) (R = Ph, **8**; R = *p*-tol **9**) are isolated as red powders in moderate yield (eq 7). Because PMe_3 reacts nearly instantaneously with W(NPh)(*o*-(Me_3SiN)$_2C_6H_4$)(py)$_2$ to form W(NPh)(*o*-(Me_3SiN)$_2C_6H_4$)(py)(PMe_3)$_2$, it is probable that this species reacts with the aldehyde to form **8** and **9**. The ^{1}H NMR spectrum of **8** exhibits a doublet at 5.91 ppm ($^3J_{PH}$ = 6.9 Hz) assignable to the aldehyde proton, while the $^{13}C\{^1H\}$ NMR exhibits a doublet at 86.2 ppm ($^2J_{PC}$ = 12.8 Hz) assignable to the carbonyl carbon. The ^{1}H NMR and $^{13}C\{^1H\}$ NMR spectra of **9** display similar resonances at similar chemical shifts. These data suggest that the aldehyde is bound to tungsten in an η^2 fashion in both **8** and **9**. Compounds **8** and **9** are air- and moisture-sensitive, while complex **8** is also temperature-sensitive, decomposing to a yellow powder within days at room temperature. It is not clear why **8** is so much more sensitive than **9**, given their similar structures.

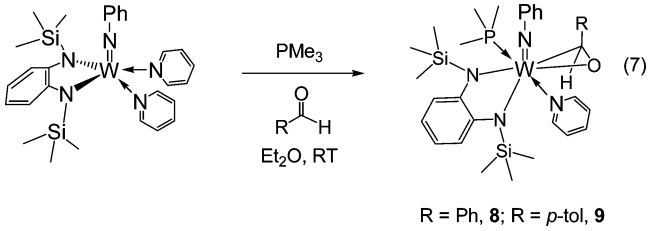

A single crystal of **9**, suitable for X-ray diffraction, was grown from a concentrated Et_2O solution. The ORTEP diagram of one of the independent molecules in the asymmetric unit of **9** is shown in Figure 6. Complex **9** adopts an octahedral geometry with the η^2-aldehyde ligand occupying a position cis to the imido ligand. In addition, the C−O bond of the aldehyde is orthogonal to the W1−N1 vector. The C7−O1 bond length is 1.356(4) Å, considerably longer than the average C−O bond length in uncoordinated aldehydes (1.20 Å), while the two W−N(amide) bond lengths are W1−N3 = 2.108(2) Å and W1−N2 = 2.138(2) Å.

Isolation of W(NPh)(*o*-(Me_3SiN)$_2C_6H_4$)(Cl)(*O*C(Me)-(CMe_3)-*o*-C_5H_4N). More mechanistic information can be garnered from the reaction between W(NPh)(*o*-(Me_3SiN)$_2C_6H_4$)(py)$_2$ and pinacolone [Me_3CC(O)Me]. A red crystalline material can be isolated from these reaction mixtures in low yield. The ^{1}H NMR spectrum of this material revealed the incorporation of only one pinacolone molecule into the product, and an X-ray crystallographic study proved these crystals to be W(NPh)(*o*-(Me_3SiN)$_2C_6H_4$)(Cl)(*O*C(Me)-(CMe_3)-*o*-C_5H_4N) (**10**).

The solid-state molecular structure of **10** is shown in Figure 7. Complex **10** exhibits an octahedral geometry around W with an essentially linear phenylimido ligand whose metrical parameters [W1a−N4 = 1.759(4) Å, W1a−N4−C1 = 160.2(4)°] are similar to those observed in **4** and **6**. The complex contains an *N*,*O* chelate formed by the coupling of one pyridine and one pinacolone. The W−O [W1a−O1 = 1.939(4) Å] and W−N(pyridine) [W1a−N1 = 2.277(5) Å] distances are similar to the related distances in **4** and **6**. The most surprising structural feature of **10** is the incorporation of a chloride ligand. The W−Cl bond length [W1a−Cl1 = 2.466(1) Å] is slightly longer than that observed for W(NPh)(*o*-(Me_3SiN)$_2C_6H_4$)Cl_2.[17] As observed in the structure of **6**, the *tert*-butyl group of the metallacycle is syn to the X^- ligand (Cl^- in this case).

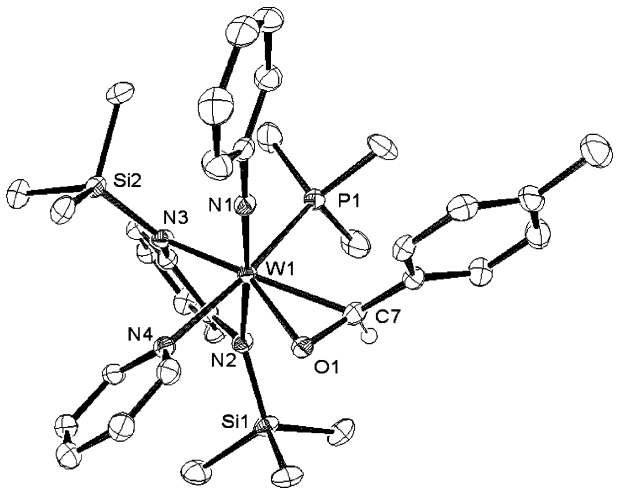

Figure 6. ORTEP diagram of W(NPh)(*o*-(Me_3SiN)$_2C_6H_4$)(PMe_3)(py)(η^2-OC(H)C_6H_4-*p*-Me) (**9**) with 50% probability ellipsoids being shown. Selected bond lengths (Å) and angles (deg): W1−N1 = 1.784(3), W1−O1 = 2.001(2), W1−N3 = 2.108(2), W1−N2 = 2.138(2), W1−C7 = 2.208(3), W1−N4 = 2.281(2), W1−P1 = 2.5347(8), O1−C7 = 1.356(4), C1−N1−W1 = 177.9(2).

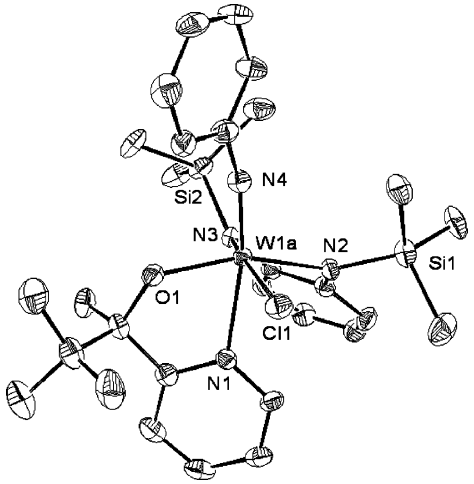

Figure 7. ORTEP diagram of W(NPh)(*o*-(Me_3SiN)$_2C_6H_4$)(Cl)(*OC*(Me)(CMe_3)-*o*-C_5H_4N) (**10**) with 50% probability ellipsoids being shown. Selected bond lengths (Å) and angles (deg): W1a−N4 = 1.759(4), W1a−O1 = 1.939(4), W1a−N3 = 1.991(5), W1a−N2 = 2.046(3), W1a−N1 = 2.277(5), W1a-Cl1 = 2.466(1), W1a−N4−C1 = 160.2(4).

The origin of the chloride ligand in **10** was not immediately clear. However, the addition of pinacolone to a diethyl ether solution of W(NPh)(*o*-(Me_3SiN)$_2C_6H_4$)(py)$_2$, followed by the introduction of excess CH_2Cl_2, provides a deep-green solution. This solution slowly turns brown-yellow, then deep-red. Cooling this mixture gave red crystals of **10** in 15% yield (eq 8). $CHCl_3$ can be substituted for CH_2Cl_2 with no improvement in yield. Interestingly, when pinacolone was added to an equimolar mixture of W(NPh)(*o*-(Me_3SiN)$_2C_6H_4$)Cl_2 and W(NPh)(*o*-(Me_3SiN)$_2C_6H_4$)(py)$_2$ in an attempt to generate **10**, a maroon powder was isolated in low yield, which proved to be W(NPh)(*o*-(Me_3SiN)$_2C_6H_4$)Cl_2(py) (**11**), the pyridine adduct of the tungsten dichloride starting material.[27]

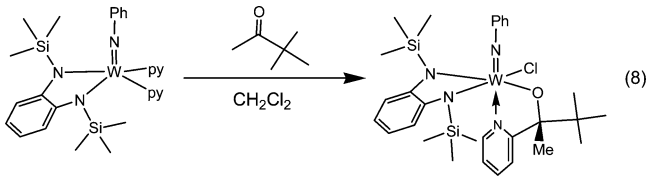

(8)

10

The isolation of **10** suggests that the tungsten hydride complex W(NPh)(*o*-(Me_3SiN)$_2C_6H_4$)(H)(*OC*(Me)(CMe_3)-*o*-C_5H_4N) is formed as an intermediate. This species then reacts with CH_2Cl_2 to form **10** and CH_3Cl. When CH_2Cl_2 is absent, no tractable products are isolated, possibly because pinacolone is too bulky to allow for the formation of an alkoxide ligand and the azaoxymetallacycle on the same metal center. This result also suggests that the formation of the axaoxymetallacycle occurs before the formation of the alkoxide ligand.

Discussion

The formation of the final double-insertion product can be explained by a number of mechanisms, as shown in Scheme 3. For instance, (a) the reaction could proceed via the formation of a pyridyl hydride intermediate, which sequentially inserts 2 equiv of aldehyde, or (b) it could proceed by the initial formation of a η^2-aldehyde complex, followed by a direct hydride transfer from pyridine to form a pyridyl alkoxide complex. Alternatively, the carbon of the η^2-aldehyde ligand could act as a nucleophile and attack the ortho carbon of pyridine to form an *N*-metalated dihydropyridine intermediate. From there, (c) H transfer to the metal to form a hydride, followed by insertion, could give the final product or (d) aldehyde could bind and direct H transfer could occur, similar to a Meerwein−Pondorf−Verley reduction.[28]

Mechanism a is consistent with the isotopic labeling studies if the C−H bond-breaking step were fast and reversible and occurred before the rate-determining step. In addition, there are many examples of pyridyl hydride species in the chemical literature, and they readily undergo insertion with unsaturated organics.[7] However, if the reaction did occur via a pyridyl hydride intermediate, one would expect the insertion of aldehyde into the W−H bond to occur before insertion into the W−C bond. This makes the formation of complex **10** harder to explain. Mechanism b is probably not operative, as it is difficult to imagine that a concerted hydrogen transfer from pyridine to aldehyde would not be rate determining and, thus, exhibit no kinetic isotope effect. Mechanism c is consistent with both the deuterium labeling studies and the isolation of complexes **8** and **9**. It also nicely accounts for the formation of **10**, which could derive from the reaction of CH_2Cl_2 with the tungsten hydride. However, it is possible that **10** forms via a completely different reaction because it does not appear that W(NPh)(*o*-(Me_3SiN)$_2C_6H_4$)(py)$_2$ reacts with 2 equiv of pinacolone under any circumstances. Mechanism d, where hydrogen transfer occurs directly to a bound aldehyde in a Meerwein−Pondorf−Verlay-style reduction, is also consistent with the available experimental evidence, but it does not explain the formation of **10** as elegantly as mechanism c.

Given this evidence, we prefer mechanism c for the reasons stated above, but also because we only see evidence for pyridyl C−H activation chemistry when there is aldehyde or ketone is present. With other unsaturated substrates, like alkenes, we only observed displacement of the pyridine ligands and not insertion.

There is literature precedent for nucleophilic attack by an acyl group at the ortho carbon of bound pyridine, followed by a 1,2 hydrogen shift.[5] The resulting product is similar to our azaoxymetallacycles. In our case, however, the nucleophile would be an η^2-aldehyde, while the hydrogen shift would be to the metal, as suggested by the deuterium labeling results. When an unsaturated substrate coordinates to the W(IV) imido diamide complexes studied here, the structures are invariably best described as W(VI) metallacycles. Thus, the butadiene complex reported in this paper is considered a $\sigma^2\pi$ butadiene complex. Assuming that a similar interaction

(27) Complex **11** can be made directly by adding pyridine to a pentane suspension of W(NPh)(*o*-(Me_3SiN)$_2C_6H_4$)Cl_2 in a much higher yield.

(28) Campbell, E. J.; Zhou, H.; Nguyen, S. T. *Org. Lett.* **2001**, *3*, 2391−2393.

Scheme 3

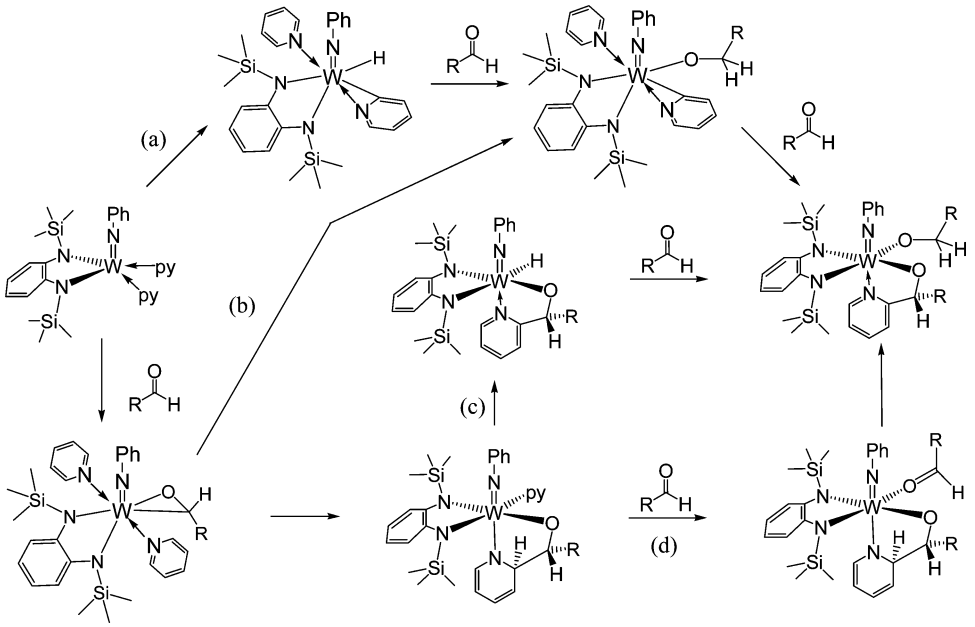

occurs between the coordinated aldehydes in **8** and **9**, the carbon atom of the aldehyde would be expected to have a considerable amount of carbanion character, which would allow it to behave as a nucleophile and attack the coordinated pyridine.

Further experiments to rule out one mechanism or the other have not been fruitful. For instance, attempts to observe a hydride intermediate by adding only 1 equiv of susbstrate have not worked, as mixtures of starting material and the double-insertion product are the only species isolated. As well, attempts to observe any transient species by NMR spectroscopy have also failed.

Summary

In this contribution, we have explored the reactivity of W(NPh)(*o*-$(Me_3SiN)_2C_6H_4$)$(py)_2$ and W(NPh)(*o*-$(Me_3SiN)_2$-C_6H_4)$(pic)_2$ with unsaturated substrates. With diphenylacetylene or olefins, displacement of the heterocyclic ligands occurs to give the simple adducts, or metallacyclic products in the case of ethylene. With some aldehydes, net substrate insertion into the ortho C−H bond of pyridine to form tungsten azaoxymetallacycle complexes is observed. Both aliphatic and aromatic aldehydes can participate in the reaction. The exact nature of the C−H bond activation step is not well understood, but mechanistic studies suggest that a tungsten pyridine η^2-aldehyde complex is formed before C−H bond activation occurs and the reaction proceeds via a metal-hydride intermediate. We have also demonstrated that, with pyridine-2-carboxaldehyde, coupling to form a diolate complex occurs. The factors that determine which reaction pathway is followed, either C−H activation or diolate formation, are not understood. Further investigation of more substrates will be necessary to reveal the factors that control this reaction. In addition, the use of new substrates may allow us to gain more insight into the C−H activation step during metallacycle formation. New developments will be reported in due course.

Experimental Section

General. All reactions and subsequent manipulations were performed under anaerobic and anhydrous conditions either under a high vacuum or an atmosphere of helium or argon. Pentane was distilled from NaK while toluene was filtered through two columns of activated alumina. Dichloromethane and pyridine were distilled from calcium hydride. C_6D_6 and pyridine-d_5 were dried over activated 4 Å molecular sieves for 24 h before use. py-d_1 was purchased from CDN Isotopes and used as received. Acetone was distilled from B_2O_3. Picoline was distilled from Na. Et_2O was distilled from Na/benzophenone. W(NPh)(*o*-$(Me_3SiN)_2C_6H_4$)$(py)_2$ and W(NPh)(*o*-$(Me_3SiN)_2C_6H_4$)$(picoline)_2$ were prepared by the literature method.[11] W(NPh)(*o*-$(Me_3SiN)_2C_6H_4$)$(py\text{-}d_5)_2$ and W(NPh)(*o*-$(Me_3SiN)_2C_6H_4$)$(py\text{-}d_1)_2$ were made in identical fashions to their unlabeled counterparts. All other reagents were purchased from commercial suppliers and used as received.

NMR spectra were recorded on a Bruker AVA300, a Varian Gemini 300, a VXR 300, or a Mercury 300 spectrometer. ^1H and $^{13}C\{^1H\}$ NMR spectra are referenced to external $SiMe_4$ using the residual protio solvent peaks as internal standards (^1H NMR experiments) or the characteristic resonances of the solvent nuclei (^{13}C NMR experiments). ^{31}P spectra were referenced to external 85% H_3PO_4. Mass spectrometry measurements were performed with a Finnigan MAT95Q hybrid sector mass spectrometer by Dr. David Powell at the University of Florida or were obtained at the U. C. Berkeley Mass Spectrometry Facility using a VG ProSpec. Elemental analyses were performed at the U. C. Berkeley Microanalytical Facility, on a Perkin−Elmer Series II 2400 CHNS analyzer.

W(NPh)(*o*-$(Me_3SiN)_2C_6H_4$)(η^2-PhC≡CPh) (1). A Young's ampule was charged with W(NPh)(*o*-$(Me_3SiN)_2C_6H_4$)$(py)_2$ (0.50 g, 0.731 mmol) and diphenylacetylene (0.13 g, 0.731 mmol). The mixture was dissolved in toluene and heated to 55 °C for 4 h, during which time the solution became yellow-brown in color. Removal of the reaction solvent in vacuo, followed by extraction with pentane, yielded a dark-yellow solution. Cannula filtration, followed by removal of the solvent in vacuo, gave 0.35 g (68% yield) of a dark-brown powder. ^1H NMR (300 MHz, 25 °C, C_6D_6): δ 0.41 (s, 18H, $SiMe_3$), 6.81 (t, 1H, phenylimido para proton), 6.97 (m, 4H, phenylimido meta and ortho protons), 7.11 (m, 5H), 7.25 (m, 2H, phenylene diamine ortho protons), 7.36 (m, 5H), 7.51 (m, 2H,

phenylene diamine meta protons). $^{13}C\{^1H\}$ NMR (75 MHz, 25 °C, C_6D_6): δ 2.38 ($SiMe_3$), 123.3, 124.7, 125.7, 128.9, 129.0, 129.2, 129.6, 130.1, 132.3, 143.1, 198.5 (C≡C). HRMS (FAB) calcd for $C_{32}H_{38}N_3Si_2W$: 704.2111 $[M + H]^+$. Found: 704.2114.

W(NPh)(*o*-(Me$_3$SiN)$_2$C$_6$H$_4$)(*C*H$_2$CH$_2$CH$_2$*C*H$_2$) (2). W(NPh)(*o*-(Me$_3$SiN)$_2$C$_6$H$_4$)(py)$_2$ (0.535 g, 0.78 mmol) and toluene were added to a Young's ampule. The sample was frozen and the flask evacuated. Upon warming to room temperature, the flask was charged with ethylene (20 psi), resulting in a color change from purple to orange. The solution was stirred for 30 min, during which time the solution changed to yellow-brown. Removal of the volatile fraction in vacuo gave a brown solid. This solid was extracted with several portions of pentane and transferred to a new vessel via a cannula filtration. Evaporation of this solution under reduced pressure gave 0.300 g (66% yield) of a yellow-brown powder. This material was determined to be W(NPh)(*o*-(Me$_3$SiN)$_2$C$_6$H$_4$)(*C*H$_2$-CH$_2$CH$_2$*C*H$_2$) (**2**) by its characteristic proton and ^{13}C NMR spectra.[14]

W(NPh)(*o*-(Me$_3$SiN)$_2$C$_6$H$_4$)(η^4-CH$_2$=C(Me)C(Me)=CH$_2$) (3). To a purple solution of W(NPh)(*o*-(Me$_3$SiN)$_2$C$_6$H$_4$)(py)$_2$ (1.00 g, 1.46 mmol) dissolved in toluene was added 2,3-dimethyl-1,3-butadiene (0.17 mL, 1.46 mmol). This mixture was heated to 60 °C for 20 h, resulting in a color change to red-brown. The volatile fraction was removed in vacuo, and the resulting brown powder was extracted with several portions of pentane and transferred to a new vessel via a filter cannula. The pentane was then removed under reduced pressure to give 0.65 g (73% yield) of **3** as a dark-brown solid. ^1H NMR (300 MHz, 25 °C, C_6D_6): δ 0.37 (s, 18H, $SiMe_3$), 1.24 (s, 6H, diene methyl), 1.31 (d, 2H, J_{HH} = 8.5 Hz, α-C*H*H), 2.17 (d, 2H, J_{HH} = 8.5 Hz, α-CH*H*), 6.85 (m, 3H, aromatic), 7.12−7.20 (m, 4H, aromatic), 7.33 (m, 2H, aromatic). $^{13}C\{^1H\}$ NMR (75 MHz, 25 °C, C_6D_6): δ 2.45 ($SiMe_3$), 18.7 (C*C*H$_3$), 50.5 (α-CH$_2$, J_{CH} = 143 Hz), 120.2 (*C*CH$_3$), 120.5, 121.0, 125.3, 127.5, 128.8, 150.0. HRMS (FAB) calcd for $C_{24}H_{38}N_3Si_2W$: 607.2035 $[M]^+$. Found: 607.2109.

W(NPh)(*o*-(Me$_3$SiN)$_2$C$_6$H$_4$)(OCH(Me)$_2$)(*O*C(Me)$_2$-*o*-C$_5$H$_4$*N*-*p*-Me) (4). To a purple solution of W(NPh)(*o*-(Me$_3$SiN)$_2$C$_6$H$_4$)-(picoline)$_2$ (0.066 g, 0.09 mmol) dissolved in toluene (1.0 mL) was added 2 equiv of acetone (13.0 μL, 0.18 mmol). The solution quickly turned green, then slowly changed to orange-brown over 20 min. After this time, the volatile fraction was removed in vacuo, and the resulting solid was dissolved in pentane (2 mL) and filtered through a column of Celite (0.5 cm × 2 cm) supported on glass wool. The resulting red-brown solution was stored at −30 °C for several hours, resulting in the deposition a brown powder. The solution was again filtered through a column of Celite and then stored at −30 °C for several weeks. This resulted in the deposition of orange crystals (0.0124 g, 18.2%). ^1H NMR (300 MHz, 25 °C, C_6D_6): δ 0.44 (s, 9H, $SiMe_3$), 0.70 (s, 9H, $SiMe_3$), 1.11 [d, 6H, J_{HH} = 6.0 Hz, OCH(*Me*)$_2$], 1.42 (s, 3H, Me), 1.54 (s, 3H, Me), 1.62 (s, 3H, Me), 4.93 [septet, 1H, OC*H*(Me)$_2$, J_{HH} = 5.9 Hz], 6.11 (d, 1H, J_{HH} = 5.8 Hz, picoline ring meta proton), 6.31 (s, 1H, picoline ring meta proton), 6.60−7.12 (m, 5H), 7.23 (m, 2H, phenylimido meta protons), 7.47 (m, 2H, phenylimido ortho protons), 8.18 (d, 1H, J_{HH} = 5.7 Hz, picoline ring ortho proton). $^{13}C\{^1H\}$ NMR (75 MHz, 25 °C, C_6D_6): δ 2.55 ($SiMe_3$), 3.71 ($SiMe_3$), 20.3 (Me), 26.6 (Me), 26.9 [OCH(*Me*)$_2$], 34.2 (Me), 75.8 [O*C*H(Me)$_2$], 118.6 (CH), 118.8 (CH), 119.5 (CH), 119.7 (picoline ring meta carbon), 119.9 (CH), 123.1 (picoline ring meta carbon), 125.9 (CH), 126.2 (phenylimido ortho carbon), 127.9 (phenylimido meta carbon), 147.2 (CH, picoline ring ortho carbon), 148.2, 150.2, 151.2, 154.7, 159.4. HRMS (EI) calcd for $C_{30}H_{46}O_2N_4Si_2W$: 734.2669 $[M]^+$. Found: 734.2608.

W(NPh)(*o*-(Me$_3$SiN)$_2$C$_6$H$_4$)(OCH$_2$Ph)(*O*CH(Ph)-*o*-C$_5$H$_4$*N*) (5). To a purple solution of W(NPh)(*o*-(Me$_3$SiN)$_2$C$_6$H$_4$)(py)$_2$ (0.0756 g, 0.11 mmol) dissolved in diethyl ether (2 mL) was added 2 equiv of benzaldehyde (23.5 μL, 0.23 mmol). The solution quickly turned forest green and then slowly became deep red. After 10 min of stirring, the volatile fraction was removed in vacuo, and the resulting red-brown powder was dissolved in pentane (2 mL) and filtered through a column of Celite (0.5 cm × 2 cm) supported on glass wool. The deep-red solution was stored at −30 °C for 24 h, resulting in the deposition of red crystals (0.0155 g). Further cooling of the solution resulted in the deposition of more crystals (0.0170 g, 36% total yield). ^1H NMR (300 MHz, 25 °C, C_6D_6): δ 0.47 (s, 9H, $SiMe_3$), 0.67 (s, 9H, $SiMe_3$), 5.65 (d, 1H, J_{HH} = 13.9 Hz, OCH*H*Ph), 5.89 (d, 1H, J_{HH} = 14.0 Hz, OC*H*HPh), 6.24−6.27 (m, 2H), 6.46 [s, 1H, OC*H*(Ph)-*o*-C$_5$H$_4$N], 6.50 (t of d, 1H, aromatic CH), 6.67−7.21 (m, 17H), 7.33 (m, 2H, phenylimido ortho protons), 8.41 (m, 1H, pyridine ring ortho proton). $^{13}C\{^1H\}$ NMR (75 MHz, 25 °C, C_6D_6): δ 2.59 ($SiMe_3$), 3.79 ($SiMe_3$), 76.0 (OCH_2), 88.5 [O*C*H-(Ph)-*o*-C$_5$H$_4$N], 118.7 (CH), 118.8 (CH), 119.5 (CH), 119.6 (CH), 120.8 (CH), 121.9 (CH), 126.0 (CH), 126.1 (CH), 126.2 (CH), 126.4 (CH), 128.0 (CH), 128.1 (CH), 128.2 (CH), 128.3 (CH), 128.8 (CH), 137.9 (CH), 144.3, 147.3 (CH, pyridine ring ortho carbon), 149.2, 149.3, 154.6, 164.7. HRMS (EI) calcd for $C_{37}H_{44}O_2N_4Si_2W$: 816.2513 $[M]^+$. Found: 816.2506. Anal. Calcd for $C_{37}H_{44}N_4O_2Si_2W$: C, 54.41; H, 5.43; N, 6.86. Found: C, 54.34; H, 5.57; N, 6.65.

W(NPh)(*o*-(Me$_3$SiN)$_2$C$_6$H$_4$)(OCHDPh)(OCH(Ph)-*o*-C$_5$D$_4$N) (5-*d*$_5$). **5**-d_5 was made in a fashion similar to that described for **5**. ^1H NMR (300 MHz, 25 °C, C_6D_6): δ 0.48 (s, 9H, $SiMe_3$), 0.71 (s, 9H, $SiMe_3$), 5.63 (s, OCD*H*Ph), 5.89 (s, OC*H*DPh), 6.47 [s, 1H, OC*H*(Ph)-*o*-C$_5$H$_4$N], 6.65−7.21 (m, 17H), 7.33 (m, 2H, phenylimido ortho protons). ^2H NMR (46 MHz, 25 °C, C_6H_6): δ 5.86 (br s), 6.27 (br m), 8.41 (br s).

W(NPh)(*o*-(Me$_3$SiN)$_2$C$_6$H$_4$)(OCH$_2$CMe$_3$)(*O*CH(CMe$_3$)-*o*-C$_5$H$_4$*N*) (6). To a purple solution of W(NPh)(*o*-(Me$_3$SiN)$_2$C$_6$H$_4$)-(py)$_2$ (0.0689 g, 0.10 mmol) dissolved in toluene (1.5 mL) was added 2 equiv of trimethylacetaldehyde (23.0 μL, 0.21 mmol). The solution quickly turned red, and after 15 min of stirring, the volatile fraction was removed in vacuo. The resulting red-brown powder was dissolved in pentane (2 mL) and filtered through a column of Celite (0.5 cm × 2 cm) supported on glass wool. The deep-red solution was stored at −30 °C for 48 h, resulting in the deposition of red crystals (0.0166 g, 21% yield). ^1H NMR (300 MHz, 25 °C, C_6D_6): δ 0.40 (s, 9H, $SiMe_3$), 0.66 (s, 9H, $SiMe_3$), 0.86 (s, 9H, CMe_3), 1.12 (s, 9H, CMe_3), 4.19 (d, 1H, J_{HH} = 11 Hz, OC*H*H-CMe_3), 4.34 (d, 1H, J_{HH} = 11 Hz, OCH*H*CMe_3), 5.20 (s, 1H, OC*H*(CMe_3)-*o*-C$_5$H$_4$N), 6.28 (m, 1H, pyridine ring meta proton), 6.50−6.81 (m, 6H), 7.06 (dd, 1H, J_{HH} = 8 Hz, J_{HH} = 1.2 Hz, diamine ring ortho proton), 7.21 (m, 2H, phenylimido meta protons), 7.37 (m, 2H, phenylimido ortho protons), 8.32 (m, 1H, pyridine ring ortho proton). $^{13}C\{^1H\}$ NMR (75 MHz, 25 °C, C_6D_6): δ 2.51 ($SiMe_3$), 3.47 ($SiMe_3$), 26.9 (C*Me*$_3$), 27.5 (C*Me*$_3$), 34.7 (*C*Me$_3$), 38.1 (*C*Me$_3$), 84.1 (OCH_2), 92.8 [O*C*H(CMe_3)-*o*-C$_5$H$_4$N], 118.3 (CH), 118.7 (CH), 118.8 (diamine ring ortho carbon), 119.3 (CH), 120.3 (CH), 121.2 (CH, pyridine ring meta carbon), 125.5 (CH), 126.0 (phenylimido ortho carbons), 128.1 (phenylimido meta carbons), 137.2 (CH), 148.5 (CH, pyridine ring ortho carbon), 149.5, 149.7, 155.1, 163.5. HRMS (EI) calcd for $C_{33}H_{52}O_2N_4Si_2W$: 776.3166 $[M]^+$. Found: 776.3139. Anal. Calcd for $C_{33}H_{52}N_4O_2Si_2W$: C, 51.02; H, 6.75; N, 7.21. Found: C, 50.84; H, 6.55; N, 6.88.

W(NPh)(*o*-(Me$_3$SiN)$_2$C$_6$H$_4$)(OCHDCMe$_3$)(*O*CH(CMe$_3$)-*o*-C$_5$D$_4$*N*) (6-*d*$_5$). 6-d_5 was made in a fashion similar to that described

for **6**. ^{1}H NMR (300 MHz, 25 °C, C_6D_6): δ 0.41 (s, 9H, $SiMe_3$), 0.67 (s, 9H, $SiMe_3$), 0.85 (s, 9H, CMe_3), 1.13 (s, 9H, CMe_3), 4.15 (s, OCD*H*CMe_3), 4.32 (s, OC*H*DCMe_3), 5.21 (s, 1H, OC*H*(CMe_3)-*o*-C_5H_4N), 6.51−7.22 (m, 8H), 7.37 (m, 2H, phenylimido ortho protons). ^{2}H NMR (46 MHz, 25 °C, C_6H_6): δ 4.13 (br s), 4.32 (br s), 6.31−7.00 (br m), 8.31 (br s).

W(NPh)(*o*-(Me_3SiN)$_2C_6H_4$)(*O*CH(C_5H_4N)CH(C_5H_4N)*O*) (7). To a purple solution of W(NPh)(*o*-(Me_3SiN)$_2C_6H_4$)(py)$_2$ (0.196 g, 0.29 mmol) in Et_2O (1 mL) was added 2-pyridine carboxaldehyde (51 μL, 0.54 mmol). The solution immediately turned deep red and copious amounts of precipitate formed. The mixture was allowed to stir for 3 h, at which point it was filtered through a column of Celite (0.5 cm × 1 cm) supported on glass wool. The Celite was subsequently rinsed with Et_2O (2 mL), and the combined filtrates were stored at −30 °C for 24 h, resulting in the deposition of red crystals (0.0174 g, 8.1% yield). ^{1}H NMR (300 MHz, −30 °C, C_7D_8): δ 0.38 ($SiMe_3$), 0.52 ($SiMe_3$), 5.91 (d, 1H, J_{HH} = 3.7 Hz, OCH), 5.95 (m, 1H, pyridine ring proton), 6.15 (d, 1H, J_{HH} = 7.6 Hz, pyridine meta proton), 6.32 (m, 1H, pyridine ring proton), 6.66 (d, 1H, J_{HH} = 3.7 Hz, OCH), 6.81 (t, 1H, J_{HH} = 10.3 Hz, phenylimido para proton), 6.93 (m, 1H, pyridine ring proton), 7.19−7.45 (m, 7H), 8.40 (d, 1H, J_{HH} = 4.2 Hz, pyridine ortho proton), 8.51 (d, 1H, J_{HH} = 5.1 Hz, pyridine ortho proton). ^{13}C{^{1}H} NMR (75 MHz, 0 °C, C_7D_8): δ 1.44 ($SiMe_3$), 2.40 ($SiMe_3$), 89.9 (OCH), 119.8 (CH), 120.1 (CH), 121.0 (CH), 121.3 (CH), 121.7 (CH), 122.8 (CH), 123.8 (CH), 125.7 (CH), 135.6 (CH), 140.9, 145.3, 147.4 (CH, pyridine ortho carbon), 148.7 (CH, pyridine ortho carbon), 154.5, 164.2, 164.4. Anal. Calcd for $C_{30}H_{37}N_5O_2Si_2W$: C, 48.71; H, 5.04; N, 9.47. Found: C, 48.73; H, 5.02; N, 9.16.

W(NPh)(*o*-(Me_3SiN)$_2C_6H_4$)(PMe_3)(py)(η^2-OCH(Ph)) (8). To a solution of W(NPh)(*o*-(Me_3SiN)$_2C_6H_4$)(py)$_2$ (0.119 g, 0.17 mmol) in Et_2O (2 mL) was added PMe_3 dropwise until an orange-brown color was achieved. Benzaldehyde (45 mg, 0.42 mmol) was added, and the solution turned deep red concomitant with the deposition of a red powder. This powder was isolated from the supernatant to give 17.6 mg of product. Pentane (2 mL) was added to the supernatant, and this solution was stored at −30 °C for 24 h, resulting in the deposition of more red powder. Total yield: 51.5 mg, 38%. ^{1}H NMR (300 MHz, 25 °C, C_6D_6): δ 0.13 (9H, $SiMe_3$), 0.23 (9H, $SiMe_3$), 0.95 (d, 9H, J_{PH} = 9.5 Hz, PMe_3), 5.91 (d, 1H, J_{PH} = 6.9 Hz, CHO), 6.59−6.95 (m, 15H), 7.13 (m, 2H, phenylimido meta protons), 7.37 (d, 2H, J_{HH} = 7.1 Hz, phenylimido ortho protons). ^{31}P{^{1}H} NMR (121 MHz, 25 °C, C_6D_6): δ −4.15 (J_{PW} = 322 Hz). ^{13}C{^{1}H} NMR (75 MHz, 25 °C, C_6D_6): δ 3.44 ($SiMe_3$), 4.32 ($SiMe_3$), 14.6 (d, J_{PH} = 27 Hz, PMe_3), 86.2 (d, J_{PH} = 12.8 Hz, CHO), 115.1 (CH), 117.7 (CH), 118.6 (CH), 120.32 (CH), 123.3 (CH), 123.8 (CH), 126.5 (CH), 127.0 (CH), 127.1 (CH), 127.2 (CH), 127.3 (CH), 138.4 (CH), 146.7, 149.5, 153.1, 156.5. Anal. Calcd for $C_{33}H_{47}N_4OPSi_2W$: C, 50.38; H, 6.02; N, 7.17. Found: C, 48.0; H, 5.61; N, 6.93. It is likely that the temperature sensitivity of **8** is responsible for the inconsistent analytical results.

W(NPh)(*o*-(Me_3SiN)$_2C_6H_4$)(PMe_3)(py)(η^2-OCH(C_6H_4-*p*-Me)) (9). To a toluene solution (2 mL) of W(NPh)(*o*-(Me_3SiN)$_2C_6H_4$)(py)$_2$ (0.214 g, 0.31 mmol) was added PMe_3 (0.0396 g, 0.52 mmol). The solution immediately turned color from purple to brown-orange. The addition of *p*-tolualdehyde (0.0381 g, 0.31 mmol) dissolved in toluene (1 mL) to this solution resulted in an immediate color change to red. After 5 min of stirring, the toluene was removed in vacuo, and the resultant red oil was rinsed with pentane (5 mL) to give 0.0577 g of red powder. The pentane washings were stored at −30 °C for 24 h, resulting in the deposition of more red powder. Total yield 0.0677 g, 27% yield. ^{1}H NMR (300 MHz, 25 °C, C_6D_6): δ 0.137 ($SiMe_3$), 0.238 ($SiMe_3$), 0.98 (d, 9H, J_{PH} = 9.6 Hz, PMe_3), 2.12 (s, 3H, CH_3), 5.95 (d, 1H, J_{PH} = 6.6 Hz, OCH), 6.68−7.12 (m, 16 H), 7.35 (d, 2H, J_{HH} = 8.1 Hz, phenylimido ortho protons). ^{31}P{^{1}H} NMR (121 MHz, 25 °C, C_6D_6): δ −3.88 (J_{PW} = 322 Hz). ^{13}C{^{1}H} NMR (75 MHz, 25 °C, C_6D_6): δ 3.45 ($SiMe_3$), 4.33 ($SiMe_3$), 14.7 (d, PMe_3, J_{PC} = 28 Hz), 20.6 (C_6H_4-*p*-*Me*), 87.5 (d, OCH, J_{PC} = 13.5 Hz), 116.1 (CH), 117.7 (CH), 118.5 (CH), 120.3 (CH), 120.4 (CH), 123.2 (CH), 123.8 (CH), 127.2 (CH), 127.8 (CH), 136.5, 140.0 (CH), 144.4, 150.1, 153.7, 157.2. Anal. Calcd for $C_{34}H_{49}N_4OPSi_2W$: C, 51.00; H, 6.17; N, 7.00. Found: C, 50.92; H, 6.14; N, 6.92.

W(NPh)(*o*-(Me_3SiN)$_2C_6H_4$)(Cl)(*O*C(Me)(CMe_3)-*o*-C_5H_4N) (10). Pinacolone (60 μL, 0.48 mmol) was added to an Et_2O (2 mL) solution of W(NPh)(*o*-(Me_3SiN)$_2C_6H_4$)(py)$_2$ (0.165 g, 0.24 mmol). The purple solution quickly turned deep green. After 1 min, excess CH_2Cl_2 was added. The solution was allowed to stir for 2 h, during which time it became deep red in color. The Et_2O was removed in vacuo, and the resulting solids were dissolved in pentane (3 mL) and filtered through a column of Celite (0.5 cm × 1 cm) supported on glass wool. The deep-red solution was stored at −30 °C for 24 h, resulting in the deposition of red crystals (0.0272 g, 15.3% yield). ^{1}H NMR (300 MHz, 25 °C, C_6D_6): δ 0.37 (s, 9H, $SiMe_3$), 0.67 (s, 9H, $SiMe_3$), 1.06 (s, 9H, CMe_3), 1.41 [s, 3H, C(O)Me], 6.23 (m, 1H, pyridine meta proton), 5.53−6.63 (m, 4H, aryl protons), 6.68 (br t, 1H, J_{HH} = 7.5 Hz, phenylimido para proton), 6.85 (m, 1H, *o*-phenylenediamine ring proton), 7.07 (d, 1H, J_{HH} = 7.8 Hz, *o*-phenylenediamine ring proton), 7.22 (t, 2H, J_{HH} = 8.2 Hz, phenylimido meta protons), 7.55 (d, 2H, J_{HH} = 6.5 Hz, phenylimido ortho protons), 8.24 (br d, 1H, J_{HH} = 5.6 Hz, pyridine ortho proton). ^{13}C{^{1}H} NMR (75 MHz, 25 °C, C_6D_6): δ 3.04 ($SiMe_3$), 3.19 ($SiMe_3$), 17.6 [C(O)*Me*], 27.2 (C*Me*$_3$), 34.8 (*C*Me$_3$), 95.0 [*C*(O)-Me], 120.3 (CH), 120.4 (CH), 120.5 (CH), 121.1 (CH), 122.4 (CH), 122.7 (pyridine ring meta carbon), 126.5 (phenylimido ortho carbon), 127.1 (phenylimido para carbon), 128.1 (phenylimido meta carbon), 138.1 (CH), 145.9, 149.9 (CH, pyridine ortho carbon), 150.4, 154.1, 159.8. HRMS (EI) calcd for $C_{29}H_{43}ClN_4OSi_2W$: 738.2174 [M]$^+$. Found: 738.2149. Anal. Calcd for $C_{29}H_{43}ClN_4OSi_2W$: C, 47.12; H, 5.86; N, 7.58. Found: C, 47.16; H, 5.60; N, 7.26.

W(NPh)(*o*-(Me_3SiN)$_2C_6H_4$)Cl_2(py) (11). To a suspension of W(NPh)(*o*-(Me_3SiN)$_2C_6H_4$)Cl_2 (0.106 g, 0.18 mmol) in pentane (1 mL) was added a pentane (1 mL) solution containing pyridine (0.026 g, 0.33 mmol). The brown suspension quickly turned purple. After 1 h of stirring, the solid was allowed to settle, and the supernatant was decanted away from a maroon powder (0.059 g, 48% yield). ^{1}H NMR (300 MHz, 25 °C, C_7D_8): δ 0.42 (s, 18H, $SiMe_3$), 6.26 (br t, 2H, J_{HH} = 5.8 Hz, pyridine meta protons), 6.53 (m, 1H, pyridine para proton), 6.56 (m, 2H, *o*-phenylenediamine ring protons), 6.65 (m, 1H, phenylimido para proton), 6.78 (m, 2H, *o*-phenylenediamine ring protons), 7.21 (m, 2H, phenylimido meta protons), 7.60 (d, 2H, J_{HH} = 7.4 Hz, phenylimido ortho protons), 8.86 (d, 2H, J_{HH} = 4.9 Hz, pyridine ortho protons). ^{13}C{^{1}H} NMR (75 MHz, 25 °C, C_7D_8): δ 1.7 ($SiMe_3$), 120.1 (CH, *o*-phenylenediamine ring carbons), 123.1 (pyridine meta carbons), 123.3 (CH, *o*-phenylenediamine ring carbons), 127.0 (CH, phenylimido ortho carbons), 128.1 (CH, phenylimido meta carbons), 128.5 (CH, phenylimido para carbon), 137.1 (CH, pyridine para carbon), 147.1, 151.8 (pyridine ortho carbons), 154.1. Anal. Calcd for $C_{23}H_{32}N_4Cl_2Si_2W$: C, 40.90; H, 4.77; N, 8.29. Found: C, 39.51; H, 4.34; N, 8.13.

X-ray Crystallography. Data for **1**, **3**, and **4** were collected at the University of Florida on a Siemens SMART PLATFORM equipped with a charge-coupled-device (CCD) area detector and a graphite monochromator utilizing Mo Kα radiation at 173(2) K.

Table 1. X-ray Crystallographic Data for Complexes **1**, **3**, **4**, **6**·$^1/_2C_5H_{12}$, **7**, **9**, and **10**·$^1/_2C_5H_{12}$

crystal data	**1**	**3**	**4**	**6**·$^1/_2C_5H_{12}$
empirical formula	$C_{32}H_{37}N_2Si_2W$	$C_{24}H_{37}N_3Si_2W$	$C_{30}H_{46}N_4O_2Si_2W$	$C_{33}H_{52}N_4O_2Si_2W \cdot {}^1/_2C_5H_{12}$
cryst habit, color	plate, red	plate, brown	plate, red	block, red
cryst size (mm)	0.23 × 0.15 × 0.03	0.17 × 0.15 × 0.03	0.20 × 0.17 × 0.17	0.20 × 0.32 × 0.40
cryst syst	monoclinic	triclinic	triclinic	triclinic
space group	$P2_1/n$	$P\bar{1}$	$P\bar{1}$	$P\bar{1}$
vol (Å^3)	3127.3(2)	2619.0(3)	1626.3(2)	1970.4(3)
a (Å)	12.5177(5)	13.1319(8)	10.0899(6)	10.1728(9)
b (Å)	15.6686(7)	14.0221(9)	11.8107(8)	10.9145(1)
c (Å)	15.9709(7)	15.0036(9)	14.1959(9)	20.648(2)
α (deg)	90	72.410(1)	95.094(1)	103.360(1)
β (deg)	93.285(1)	84.247(1)	97.433(1)	93.943(1)
γ (deg)	90	89.938(1)	102.417(1)	115.795(1)
Z	2	2	2	2
fw (g/mol)	703.68	607.60	734.74	819.8
density (calcd) (Mg/m^3)	1.495	1.541	1.500	1.370
abs coeff (cm^{-1})	3.795	4.517	3.657	3.026
F_{000}	1408	1216	744	834
radiation	Mo Kα, 0.710 73 Å	Mo Kα, 0.710 73 Å	Mo Kα, 0.710 73 Å	Mo Kα, 0.710 73 Å
		Data Refinement		
final R indices[a]	$R_1 = 0.021$, w$R_2 = 0.049$	$R_1 = 0.030$, w$R_2 = 0.066$	$R_1 = 0.056$, w$R_2 = 0.092$	$R_1 = 0.025$, w$R_2 = 0.068$
largest diff. peak and hole (e$^-$Å^{-3})	0.51 and −0.33	0.742 and −0.841	1.30 and −1.07	1.83 and −1.41

crystal data	**7**	**9**	**10**·$^1/_2C_5H_{12}$
empirical formula	$C_{30}H_{37}N_5O_2Si_2W$	$C_{34}H_{49}N_4OPSi_2W$	$C_{29}H_{43}ClN_4OSi_2W \cdot {}^1/_2C_5H_{12}$
cryst habit, color	rectangular slab, red	irregular, red	multifaceted block, red
cryst size (mm)	0.04 × 0.08 × 0.14	0.10 × 0.16 × 0.10	0.18 × 0.22 × 0.34
cryst syst	tetragonal	monoclinic	orthorhombic
space group	I_1/a	$P2_1/n$	$Pbc2_1$
vol (Å^3)	12484(1)	7231.6(5)	7014.7(5)
a (Å)	30.267(2)	20.1063(9)	9.3024(4)
b (Å)	30.267(2)	12.3263(5)	23.567(1)
c (Å)	13.6276(7)	29.989(1)	31.998(1)
α (deg)	90	90	90
β (deg)	90	103.343(1)	90
γ (deg)	90	90	90
Z	16	8	8
fw (g/mol)	739.68	800.77	775.23
density (calcd) (Mg/m^3)	1.574	1.471	1.468
abs coeff (cm^{-1})	3.813	3.337	3.467
F_{000}	5920	3248	3144
radiation	Mo Kα, 0.710 73 Å	Mo Kα, 0.710 73 Å	Mo Kα, 0.710 73 Å
		Data Refinement	
final R indices[b]	$R_1 = 0.039$, w$R_2 = 0.090$	$R_1 = 0.028$, w$R_2 = 0.063$	$R_1 = 0.039$, w$R_2 = 0.078$
largest diff. peak and hole (e$^-$Å^{-3})	2.35 and −0.84	1.28 and −1.04	1.54 and −0.84

[a] Number of observed reflections: For **1**, 7161 ($I_o > 2\sigma I_o$), $R_1 = \sum(||F_o| - |F_c||)/\sum|F_o|$, w$R_2 = [\sum w(|F_o|^2 - |F_c|^2)^2/\sum wF_o^4]^{1/2}$, $w = [\sigma^2F_o^2 + (0.037p)^2 + 0.31p]^{-1}$, $p = [F_o^2 + 2F_c^2]/3$. For **3**, 11 758 ($I_o > 2\sigma I_o$), $R_1 = \sum(||F_o| - |F_c||)/\sum|F_o|$, w$R_2 = [\sum w(|F_o|^2 - |F_c|^2)^2/\sum wF_o^4]^{1/2}$, $w = [\sigma^2F_o^2 + (0.037p)^2 + 0.31p]^{-1}$, $p = [F_o^2 + 2F_c^2]/3$. For **4**, 7205 ($I_o > 2\sigma I_o$), $R_1 = \sum(||F_o| - |F_c||)/\sum|F_o|$, w$R_2 = [\sum w(|F_o|^2 - |F_c|^2)^2/\sum wF_o^4]^{1/2}$, $w = [\sigma^2F_o^2 + (0.0265p)^2]^{-1}$, $p = [F_o^2 + 2F_c^2]/3$. For **6**·$^1/_2C_5H_{12}$, 8897 ($I_o > 2\sigma I_o$), $R_1 = \sum(||F_o| - |F_c||)/\sum|F_o|$, w$R_2 = [\sum w(|F_o|^2 - |F_c|^2)^2/\sum wF_o^4]^{1/2}$, $w = [\sigma^2F_o^2 + (0.0450p)^2 + 1.9216p]^{-1}$, $p = [F_o^2 + 2F_c^2]/3$. [b] Number of observed reflections: For **7**, 6060 ($I_o > 2\sigma I_o$), $R_1 = \sum(||F_o| - |F_c||)/\sum|F_o|$, w$R2 = [\sum w(|F_o|^2 - |F_c|^2)^2/\sum wF_o^4]^{1/2}$, $w = [\sigma^2F_o^2 + (0.0473p)^2 + 43.7649p]^{-1}$, $p = [F_o^2 + 2F_c^2]/3$. For **9**, 17 910 ($I_o > 2\sigma I_o$), $R_1 = \sum(||F_o| - |F_c||)/\sum|F_o|$, w$R_2 = [\sum w(|F_o|^2 - |F_c|^2)^2/\sum wF_o^4]^{1/2}$, $w = [\sigma^2F_o^2 + (0.0191p)^2 + 9.5164p]^{-1}$, $p = [F_o^2 + 2F_c^2]/3$. For **10**·$^1/_2C_5H_{12}$, 16 526 ($I_o > 2\sigma I_o$), $R_1 = \sum(||F_o| - |F_c||)/\sum|F_o|$, w$R2 = [\sum w(|F_o|^2 - |F_c|^2)^2/\sum wF_o^4]^{1/2}$, $w = [\sigma^2F_o^2 + (0.0381p)^2 + 3.3258p]^{-1}$, $p = [F_o^2 + 2F_c^2]/3$.

For each, a hemisphere of data (1381 frames) was collected using the ω-scan method (0.3° frame width). The first 50 frames were remeasured at the end of data collection to monitor the instrument and crystal stability (maximum correction on I was <1%). Absorption corrections by integration were applied on the basis of measured indexed crystal faces. The structures were solved by the direct methods in SHELXTL5[29] and refined using full-matrix least squares on F^2. The non-H atoms were treated anisotropically, whereas the hydrogen atoms were calculated in ideal positions and were riding on their respective carbon atoms. For **1**, a total of 349 parameters were refined in the final cycle of refinement using 7161 reflections with $I > 2\sigma(I)$ to yield R1 and wR2 values of 2.08% and 4.87%, respectively. For **3**, the asymmetric unit consisted of two independent molecules. A total of 589 parameters were refined in the final cycle of refinement using 11 758 reflections with $I > 2\sigma(I)$ to yield R1 and wR2 values of 3.00% and 6.55%, respectively. For **4**, a total of 367 parameters were refined in the final cycle of refinement using 7205 reflections with $I > 2\sigma(I)$ to yield R1 and wR2 values of 5.59% and 9.23%, respectively.

The crystal structures of compounds **6**, **7**, **9**, and **10** were determined as follows, with exceptions noted in subsequent paragraphs. The crystal was mounted in a nylon cryoloop from

(29) Sheldrick, G. M. *SHELXTL5*; Nicolet XRD Corp.: Madison, WI, 1995.

Paratone-N oil under an argon gas flow. The data were collected on a Bruker SMART APEX II CCD diffractometer, with a KRYO−FLEX liquid nitrogen vapor cooling device. All data were collected at 141 K. The instrument was equipped with a graphite monochromatized Mo Kα X-ray source ($\lambda = 0.710\,73$ Å), with MonoCap X-ray source optics. A hemisphere of data was collected using ω scans, with 5-s frame exposures and 0.3° frame widths. Data collection and initial indexing and cell refinement were handled using APEX II software.[30] Frame integration, including Lorentz-polarization corrections, and final cell parameter calculations were carried out using SAINT+ software.[31] The data were corrected for absorption using the SADABS program.[32] The decay of reflection intensity was monitored via an analysis of redundant frames. The structure was solved using direct methods and difference Fourier techniques. All hydrogen atom positions were idealized and rode on the atom they were attached to. The final refinement included anisotropic temperature factors on all non-hydrogen atoms. Structure solution, refinement, graphics, and creation of publication materials were performed using SHELXTL.[33]

For compound **6**, a total of 426 parameters were refined in the final cycle of refinement using 8897 reflections with $I > 2\sigma(I)$ to yield R1 and wR2 values of 2.53% and 6.76%, respectively. In addition, an *n*-pentane molecule was found to occupy an inversion center in the lattice, with the inversion center lying on the midpoint between the third and fourth carbon atoms of the *n*-pentane molecule. This disorder was modeled as two full occupancy carbon atom positions (C35 and C36) and one one-half occupancy carbon atom position (C34). Carbon atoms C34, C35, and C36 were refined anisotropically, but without their associated hydrogen atom positions. For **7**, a total of 375 parameters were refined in the final cycle of refinement using 6060 reflections with $I > 2\sigma(I)$ to yield R1 and wR2 values of 3.91% and 8.97%, respectively. For **9**, a total of 803 parameters were refined in the final cycle of refinement using 17 910 reflections with $I > 2\sigma(I)$ to yield R1 and wR2 values of 2.75% and 6.28%, respectively. For compound **10**, a total of 761 parameters (with one restraint) were refined in the final cycle of refinement using 16 526 reflections with $I > 2\sigma(I)$ to yield R1 and wR2 values of 3.91% and 7.78%, respectively. In addition, after all atomic positions were assigned, and refined anisotropically to convergence, a significant residual peak ($\sim$15 e^{-}Å^{-3}) remained approximately 2.1 Å away from the tungsten atom. Since the peak occurred at a chemically anomalous position, it was assumed to result from a small twin. This residual peak was observed in each of the crystallographically independent tungsten molecules in the structure. The residual peaks were refined as partial occupancy tungsten atoms, with variable site-occupancy factors. The sum of the site-occupancy factors for the major and minor tungsten components was fixed at 1.0 for each independent molecule. In addition, the occupancies of the major and minor components of each independent molecule were constrained to be equivalent. This final refinement resulted in a site occupancy of 6.16(7)% for the minor twin component. A summary of relevant crystallographic data is found in Table 1, and full details of all crystallographic analyses are provided in the Supporting Information.

Acknowledgment. We are grateful to the National Science Foundation (Grant No. CHE-0094404) and the LDRD program at Los Alamos National Laboratory for support of this work. T.W.H. acknowledges NSERC (Canada) for a postdoctoral fellowship. We also acknowledge Corey B. Wilder for preliminary studies in this area.

Supporting Information Available: Complete details of the X-ray crystallographic studies as CIF files. This material is available free of charge via the Internet at http://pubs.acs.org.

IC0511367

(30) *APEX II*, version 1.08; Bruker AXS, Inc.: Madison, WI, 2004.
(31) *SAINT+*, version 7.06; Bruker AXS, Inc.: Madison, WI, 2003.
(32) Sheldrick, G. M. *SADABS*, version 2.03; University of Göttingen: Göttingen, Germany, 2001.
(33) *SHELXTL*, version 5.10; Bruker AXS, Inc.: Madison, WI, 1997.